Journal of Building Engineering 97 (2024) 110652

Contents lists available at ScienceDirect

Journal of Building Engineering

journal homepage: www.elsevier.com/locate/jobe

Performance of self-compacting concrete with treated rice husk ash at different curing temperatures

Ayman Almutlaqah [a,b], Abdullah Alshahrani [a,b], Riccardo Maddalena [a], Sivakumar Kulasegaram [a,*]

[a] School of Engineering, Cardiff University, Cardiff, CF24 3AA, UK
[b] Civil Engineering Department, College of Engineering, Najran University, Najran, Saudi Arabia

ARTICLE INFO

Keywords:
Curing temperature
Fresh properties
Heat of hydration
Compressive strength development
Porosity
Maturity

ABSTRACT

Self-compacting concrete (SCC) is currently gaining traction as a replacement to conventional vibrated concrete. Its distinct microstructure leads to varied mechanical behaviour under different curing temperatures. In the past various supplementary cementitious materials (SCMs) were used in SCC to investigate their respective effects on the performance. However, there has been no systematic studies conducted to determine the effect of different curing temperature on the sensitivity reaction of rice husk ash (RHA) in SCC. This research focuses on high-strength SCC with SCMs such as RHA, silica fume (SF), fly ash (FA), and ground granulated blast-furnace slag (GGBS), exploring their applicability for concrete structures under varying curing temperatures. Heat of hydration, compressive strength and open porosity of SCC specimens were assessed at various temperature. Results indicate high curing temperatures expedite the hydration and pozzolanic reaction, refining the microstructure and increasing the early-age concrete strength, but compromising the long-term performance, potentially mitigated by the use of SCMs. Conversely, lower curing temperature, impedes hydration leading to gradual strength gain, particularly with SCMs, yet yielding significant strength increases at later concrete age. SCMs presence and curing temperature significantly influence maturity function-based strength predictions, impacting strength trends in the samples studied.

1. Introduction

The introduction of self-compacting concrete (SSC) has been an important step in concrete development due to its high flowability and good compaction without the need for additional vibration. This makes SCC ideal for structures with dense reinforcement [1,2]. Its adoption is increasing globally, particularly for heavy reinforced concrete applications, and it is anticipated that it will gradually supplant vibrated concrete across a range of uses, including high-rise constructions. However, the growing requirement for concrete in high-rise construction may make normal-strength SCC unfavourable choice to meet the needs [2–5].

Despite its benefits, SCC requires a greater volume of cement compared to conventional concrete [1]. This presents a sustainability challenge as cement is the main factor responsible for CO_2 emissions during concrete production [6]. Therefore, the addition of supplementary cementitious materials SCMs as a replacement for cement is necessary to enhance the sustainability. However, this can affect the fresh properties, hydration kinetic and hardened characteristics of SCC [7–10].

* Corresponding author.
E-mail address: KulasegaramS@cardiff.ac.uk (S. Kulasegaram).

https://doi.org/10.1016/j.jobe.2024.110652
Received 5 June 2024; Received in revised form 25 August 2024; Accepted 1 September 2024
Available online 10 September 2024

The reactivity of cement, known as hydration, occurs immediately after the cement is mixed with water, yielding calcium hydroxide (CH) and calcium silicate hydrate (C-S-H), which is responsible for the strength development [11]. The pozzolanic reaction is the reaction of silica oxide (SiO_2) of supplementary materials with the CH that is produced from the hydration reaction of cement with water (H_2O) [12]. This can lead to the formation of extra C-S-H phase and improve the hydration of the cement, which in turn improves the performance of the concrete [13–16]. Due to the different chemical compositions and physical properties of the pozzolanic materials, each type of material offers a distinctive reactivity. Generally, the pozzolanic materials can be categorized into two groups [17]: (a) highly-reactive material, (b) low-or moderately-reactive material. This difference in reactivity not only occurs during standard curing temperature but also can be more significant at differing temperatures [18–21].

With maturity, the concrete experiences different ambient temperatures and different internal temperatures generated by the hydration [22–25]. The compressive strength of the concrete, primarily attributed to the hydration of cement, is typically considered an indicator of its performance [26,27]. The early strength characteristic of the concrete is significant since it primarily affects the long-term strength and performance of the concrete. Typically, the concrete gains faster strength with higher curing temperatures. However, high curing temperatures can lead to attenuation strength growth over the time. Conversely, curing concrete at low temperatures can hinder its initial strength development, but yield greater strength at a later time [25,28–30].

Many studies have reported the effects of temperature curing on the behaviour of conventional concrete [14,19–21,30–32], and research are still being carried out. There is a perceptible gap in knowledge regarding the performance of SCC containing SCMs under varying curing temperatures. Therefore, any conclusions drawn from previous studies are only viable in the particular cases that have been investigated. SCC is formulated using materials comparable to vibrated concrete, but with varying mix ratio [33–35]. The different mix proportion requirement in SCC, alongside the omission of vibration during casting, can cause distinctive impacts of temperature curing on the hydration process that would subsequently affect its microstructure [36] and hardened properties [5,37,38].

A study to test the influence of temperature on SCC properties has been reported [39]. Different SCC samples with strength classes between 25 and 85 MPa were cured at temperatures of 20, 40, 60 and 80 °C. The replacement levels of fly ash in the binder were 0 and 20 %. The maximum total curing time until the test in this study was approximately 2 days [39]. The conclusion drawn from the study indicated that the pores of SCC appeared coarser when it is placed in heat treatment.

Soutsos et al. [37] investigated the impact of different curing temperatures on the behaviour of strength gain of SCC up to 28 days. The cement binder was partially substituted by 30 % GGBS and limestone powder, respectively, with a target strength of 60 MPa. The results showed an improvement in early-age strength at higher curing temperatures, whilst it detrimentally affected the later-age strength. However, later-age strength was less influenced by temperature for the samples containing GGBS. Boukhelkhai et al. [40], reported similar behaviour further affirming the contribution of SCMs to alleviate the negative influence of high temperatures over time.

Benaicha et al. [41] examine the strength evolution for up to 7 days of high-strength SCC placed at varying temperatures. This was undertaken to confirm the safe accomplishment of construction operations by a maturity technique when applying SCC in construction scenarios.

Previous studies concentrated on the behaviour of early-age strength gain of SCC up to 28 days. The increase in concrete strength due to additional hydration of SCMs after 28 days can improve the safety of the structure. However, more studies are required to investigate the strength development of SCC with SCM in the long term. In addition, silica fume (SF), fly ash (FA) and ground granulated blast-furnace slag (GGBS) have been widely used as a replacement of cement in SCC over the years. Therefore, other industrial by-products such as rice husk ash (RHA) which has a continual increase in a production [42], and possess suitable chemical compositions, make it a feasible alternative SCMs for use in SCC [43].

To the best of the author's knowledge, the behaviour of SCC, including RHA, has not been investigated when subjected to varying curing temperatures. This research findings aim to enhance the existing knowledge regarding the long-term strength gain of high-strength SCC with SCMs at different curing temperatures. The novelty of this study lies in its investigation of high-strength SCC incorporated with treated RHA, assessing how different curing temperatures influence its properties, in order to enhance the reliability of SCC applications in construction scenarios. To fulfil the goal, the reference SCC mix was prepared as a cement binder, while the residual mixes had 10 % RHA, 10 % SF, 20 and 40 % FA, 20 and 40 % GGBS blended with cement. The fresh properties of all SCC mixes

Table 1
Chemical composition and physical characteristics of ordinary Portland cement (PC, type I 52.5 MPa) and SCMs employed.

Composition	Cement	SF	FA	GGBS	RHA
SiO_2 (%)	19.69	85	53.10	34.34	80
Al_2O_3 (%)	4.32	–	20.64	12.25	0.15
Fe_2O_3 (%)	2.85	–	8.93	0.32	0.01
CaO (%)	63.04	1	6.12	39.90	0.98
K_2O (%)	0.74	–	2.17	0.45	2.09
Na_2O (%)	0.16	4	1.68	0.41	0.07
MgO (%)	2.17	–	1.79	7.70	0.40
SO_3 (%)	3.12	2	1.93	0.23	0.80
TiO_2 (%)	0.33	–	0.90	0.65	0.01
Specific gravity	3.15	2.20	2.40	2.40	2.10
Loss on ignition (%)	3.03	4	2.93	0.34	13.49

were investigated by a slump flow and J-ring tests. A total of 756 SCC specimens were prepared and positioned in the tank curing environment set at 10, 20, 35 or 50 °C. Compressive strength, hydration and porosity were investigated to understand the effects of heat treatment on SCC mixes. The prediction of the strength development of the concrete was also tested. The study results evaluated the applicability and robustness of the tested mixes, hence promoting the adoption of eco-friendly and sustainable SCC in construction.

2. Experimental description

2.1. Materials

Portland cement (PC) (CEM I 52.5 N) as per the specifications of (EN 197-1) [44], SF, FA, GGBS and RHA were used with specific gravities of 3.15, 2.2, 2.4, 2.4 and 2.1, respectively. RHA was thermally treated at 400 °C for 6 h and ground. The chemical compositions and physical properties of PC and SCMs are provided by the suppliers and listed in Table 1. For the coarse aggregate, crushed limestone with a specific gravity of 2.65 and maximum particle size of 10 mm was used. The fine aggregate consisted of natural river sand with a specific gravity of 2.55 and particle sizes smaller than 2 mm. Limestone dust with a specific gravity of 2.6 and comparable particle size to the river sand was used as a replacement for about 30 % of the river sand. The particle size distribution curves of coarse and fine aggregate are presented in Fig. 1. For the mixes, tap water was used. To attain the required workability of SCC mixes with low water content, a water reducer was added. Poly-Aryl-Ether (MasterGlenium ACE 499) type superplasticizer according to (BS EN 934-2) [45] was used with a specific gravity of 1.07. The water-to-cement (W/C) ratio of 0.40 was chosen for formulating the studied mixes to attain the desired compressive strength of 70 MPa after a curing period of 28 days, following the mix design method proposed by Alshahrani et al. [46]. The dosage levels of PC replacement in the binder by FA or GGBS was 20 and 40 % by weight for each, whereas the dosage level of SF or RHA was 10 %. It may be noted that using more than 10 % of SF or RHA in the binder was not found to provide desirable fresh properties in which the mixes meet the SCC standards. Due to the cellular structure of RHA and the fineness of SF, a higher water content is needed. Thus, the amount of superplasticiser for the mixes containing SF or RHA was adjusted to achieve the self-compacting characteristics [47]. The mix proportions are given in Table 2. The control SCC is referred as RF. The other SCC mixtures were identified by label X-Y, where X represents the type of blended material in the paste, and Y shows the level of replacement of cement by the pozzolanic materials in the binder.

2.2. Mixing process

The constituents of SCC were mixed by placing coarse aggregate, followed in sequence by PC, fine aggregate, SCM, water and superplasticizers. The aggregates were oven-dried before use. Initially, coarse aggregate was blended for a minute in mixer followed by PC blended with coarse aggregate for another minute. Subsequently, the river sand and limestone dust were introduced together into the mixture and blended for roughly 2 min to guarantee uniform consistency through the mixes. Thereafter, SCM was placed and mixed for 1 min. A portion of the SP, equating to one-third of its total amount, was mixed with water and then incrementally added to the mixture in two stages. The remaining SP was then incorporated during the mixing process. Finally, the mixing process proceeded for an additional 6 min, leading to a full mix duration of 11 min. Before moulding the concrete, different types of fresh tests were performed to investigate the self-compatibility properties of the conducted mixes such as the slump flow test and J-ring test. The equipment consisted of a slump cone and baseplate made from steel for the slump flow test, and a ring containing different numbers of vertically positioned reinforcing bars, slump cone and steel baseplate as shown BS EN 12350-8 and BS EN 12350-12 [48,49].

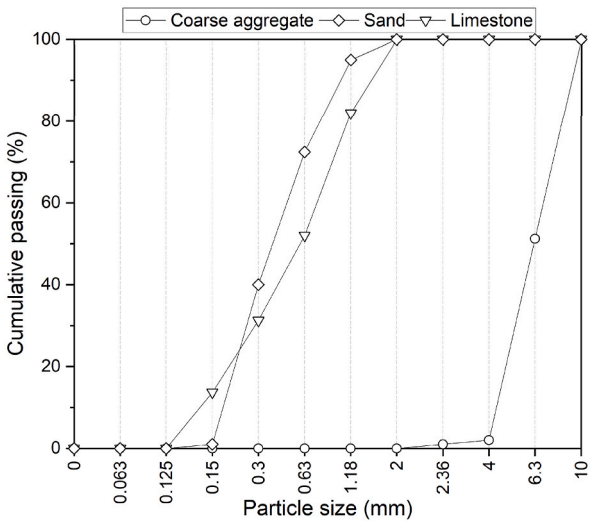

Fig. 1. Particle size distribution of aggregate.

Table 2
Mix proportion of the starting materials in the studied mixes.

Mix ID	PC	Mix proportion (kg/m^3)								
		Binder materials				Aggregate			Water	SP
		RHA	FA	GGBS	SF	Fine		Coarse		
						Sand	Limestone			
RF	514.1	–	–	–	–	525	225	833	205.6	3.3
SF-10	462.6	–	–	–	51.4	525	225	820.5	205.6	5.4
FA-20	411.2	–	102.7	–	–	525	225	810	205.6	3.5
FA-40	308.4	–	205.6	–	–	515.3	220.9	796.9	205.6	3
GGBS-20	411.2	–	–	102.7	–	525	225	810	205.6	3.5
GGBS-40	308.4	–	–	205.6	–	515.3	220.9	796.9	205.6	3
RHA-10	462.6	51.4	–	–	–	525	225	820.5	205.6	3.6

2.3. Heat of hydration

The hydration of cement pastes and that of corresponding concrete might not necessarily be the same. Most isothermal calorimeters are not applicable for monitoring cement hydration in concrete systems because of the limited size of the samples. In order to demonstrate the effects of using SCM on the hydration of SCC, the measurements were conducted using an isothermal calorimeter (Calmetrix I-Cal 8000 HPC) [50], conforming with ASTM C1072- 2017 [51], and with curing temperature settings of 10, 20, 35 and 50 °C, respectively. Its large sample size, exceeding previous studies [52–54], can directly monitor the hydration outputs of the concrete with a high level of accuracy. At each setting temperature, after the concrete was mixed, about 270g of the sample was relocated to a sample holder, which was then sealed, and placed in the calorimeter. Each test was conducted in duplicate runs for a duration of up to 100 h following the guidelines in Ref. [51]. SCM materials were substituted with cement at different dosage levels to investigate their influence on the hydration process. The heat measurement was taken every 1 min for a total period of 100 h. The heat rate of the studied samples was then calculated following ASTM C1897- 2020 [55].

2.4. Compressive strength test

The concrete was cast into cubic moulds with a 10 cm dimension and compacted solely by the weight of the sample without using a vibration table. The samples with their moulds were covered and enveloped using a polyethene before being immersed in water tanks set to varying curing temperatures up to 50 °C to assess the impacts of different temperatures on the rate of strength development. The specimens were removed from their moulds after first day and immediately returned to their respective tanks. The compressive strength was performed as per BS EN 12390-3 [56] at 1, 3, 7, 14, 28, 56 and 90 days after the concrete casting in triplicate.

2.5. Open porosity test

Following the curing period for early age (3 days) and later-age (90 days) of the concrete, the specimens for porosity investigation were oven-dried at 60 °C for approximately 3 days until the weight recorded did change by more than 0.2 % over a period of 3 h [57]. The open porosity measurements were carried out based on the open porosity and density method proposed by interlaboratory comparison of hygric properties of porous building materials (HAMSTAD) [58].

3. Result and discussion

3.1. Fresh state

When in its fresh state, concrete conforms to three main criteria: the capacity to fill the space, the ability to pass through narrow areas without blockages, and resistance to segregation [59], it is said to be SCC. The fresh state of SCC mixes is evaluated by different fresh tests described by EFNARC, including the slump flow, slump flow time (t_{50}), and J-ring tests. Table 3 summarised the fresh test results. All the mixes exhibited an acceptable slump flow spread diameter (550–850 mm) and slump flow time (t_{50}) according to Ref. [60]. The capability of SCC mixes to navigate through reinforcement bars was assessed using J-ring test [49]. The results indicated

Table 3
The fresh test results of the studied mixes.

Mix label	Slump flow spread (mm)	t_{50} (s)	Slump flow spread-J-ring flow spread (mm)	The difference in vertical levels between the concrete within and outside the ring (mm)
RF	645	1.78	45	10
SF-10	660	2	50	10
FA-20	690	1.47	15	7.5
FA-40	720	1	15	2.5
GGBS-20	670	2.3	20	4
GGBS-40	740	1.7	50	4
RHA-10	665	2.3	40	8.8

there was no blockage observed in the examined mixes as per [60,61]. By visual inspection, it was verified that the mixes exhibited no indication of segregation. It is worth mentioning that mixes that did not achieve the SCC standards were eliminated and not considered in this study. The effects of including the supplementary materials as a part of cement on their workability are considerable in terms of their nature and dosage.

The fineness of SF [62] and the porous structure along with the irregular shaped particles of RHA [63] caused a greater area of the particle to be conducted to the water, resulting in more absorption. This caused a decrease in the amount of free water in the concrete, which led to a decrease in workability. This brings to light the fact that a greater volume of superplasticizer was required to meet the SCC standards. These observations are comparable with those indicated in Refs. [7,43,64,65].

FA has a spherical particle shape and a lower density than cement. Substituting cement with FA and GGBS led to a larger amount of paste, which in turn decreased the friction between paste and aggregate resulting in an increase in workability. This trend is an agreement between several earlier studies [47,66–69]. Therefore, a lower volume of superplasticizer was needed to achieve SCC standards.

3.2. Heat of hydration of SCC

It is evident that the reaction rate relies on the chemical compositions driven by Ca/Si ratios [10], physical properties related to the size of particles and their packing [70], the curing temperature [16] and diffusion processes at a later age [11,71].

The inclusion of materials that have a greater quantity of SiO_2 causes more consumption of (CH) [10,14]. Hence, rapid pozzolanic reactions can be produced. Furthermore, with finer particles, a greater area of the particle is exposed and conducted to water. This results in a greater reaction between particles, which can improve the strength. The amount of filler involved can also significantly influence the reaction process, since the possibility for the formation of nucleation sites for the C-S-H phase can be increased with the inclusion of a greater volume of the paste [70,72]. The rate of the hydration reaction becomes high with high-temperature curing and vice versa. Eventually, the diffusion of the water and dissolved elements through C-S-H might also affect the reaction [11,71].

When compared with cement, pozzolanic materials normally have more silica, less calcium, and different physical properties (see Table 1). This highlights the fact that different products can be formed from hydration when they are blended with cement. This affects the various stages of hydration; that is, the induction period, the acceleration period, the deceleration period and the diffusion period. The effects on these periods would be greater with different curing temperatures [21]. This will significantly affect the second step, during which the properties of hardened concrete such as strength and durability [10].

The hydration reaction occurs immediately after the water has been mixed with cement (Fig. 2a and Fig. 2b). Fig. 2a shows the heat flow of cement, SF, FA, GGBS and RHA cured at standard temperature. It can be seen that the temperature rises of the control sample were reached at about 13 h.

For SCC specimens incorporating FA or GGBS, it was observed that the heat peaks generated was lower than the control sample during the measurement interval. Additionally, these peaks were more delayed with higher levels of replacement of FA or GGBS. This indicates that the pozzolanic reaction begins to take place during the hydration process. FA and GGBS have an additional source of CaO, which leads to the production of some CH from the hydration reaction. Therefore, more time is needed for the SiO_2 to consume CH [10,72–74]. This can explain the low and slow reaction of FA and GGBS, which is reflected in slow strength development. FA contains large amounts of SiO_2 and Al_2O_3 and can also contain a little CaO. This is variable, depending on the source of FA [71]. Incorporating Al ions with C-S-H to form C-A-S-H, which has a low Ca/Si ratio, might lead to an increase in the solubility of Ca [10,73,74]. Nevertheless, FA reacts in a heterogeneous manner with cement and might require a much longer time to be homogenised [74]. Furthermore, the diffusion process starts to dominate after a short time of the FA reaction [75]. In contrast, GGBS has less SiO_2 and Al_2O_3 but more CaO than FA [10]. When the substitution level of FA or GGBS is high, the reaction becomes slower due to the reduction of alkali content (pH), leading to a decrease in the solubility process between the silicates and pH [10,72]. Furthermore, the diffusion effect becomes more dominant with increasing replacement levels of cement by FA or GGBS [16,71].

Specimens with SF or RHA exhibited higher and earlier heat than FA and GGBS samples. SF is a material with high pozzolanic activity owing to its high silicate composition, very fine particle size and low density, which enhance the filler effects [10,76].

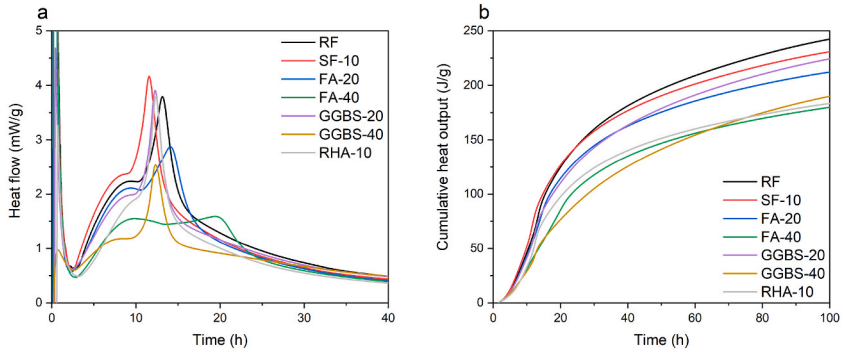

Fig. 2. Heat of hydration of all mixes using an isothermal calorimeter at 20 °C, (a) heat flow (mW/g) normalised by the weight of binder (plotted only for the first 40 h for detailed view), (b) total cumulative heat flow (J/g) normalised by the weight of the binder.

Including materials that are rich in silicate leads to more consumption of CH and can contribute to an acceleration of the reaction [14]. This can explain why, in our results, SF-10 was more pronounced in its reaction and achieved higher and earlier peak temperatures than the control sample. Hence, rapid development of strength occurred. In contrast, the hydration process of the mixes including RHA in cement binder is more complex when contrasted with other pozzolanic materials, mainly due to the porous structure of RHA particles including absorption and release of the water [77].

RHA affects the hydration process via the following main mechanisms: the pozzolanic effect, the porous structure effect and the internal curing effect [78,79]. The high silica content of RHA leads to a reduction in the Ca/Si ratio and improvements in the formation of C-S-H products. This, in turn, has the potential to enhance the hydration reaction [78]. However, the pozzolanic reaction between RHA and cement is influenced by the porous structure of RHA. During mixing, the pores of the particles can absorb some free water, causing a reduction of the water in the system and decreasing the early stage of hydration for cement [78,79]. The stored water in the porous particles of RHA can also affect hydration through the ongoing release of water from RHA (internal curing effect). When the moisture level within the matrix decreases, water is released from the pores of RHA particles, facilitating additional hydration at a later age [78,79].

During the acceleration period of all the studied specimens, the main peak appears irregular, exhibiting two peaks attributing to the varying reactivity of different mineral components within cement. The initial peak which induced by a higher hydration rate of C_3S, causing a significant release of heat. Subsequently, the rate of the heat evolution starts to diminish as the hydration of C_3S hinders. In the interim between the initial and subsequent peaks, the less reactive C_2S initiates its involvement in the hydration process. The

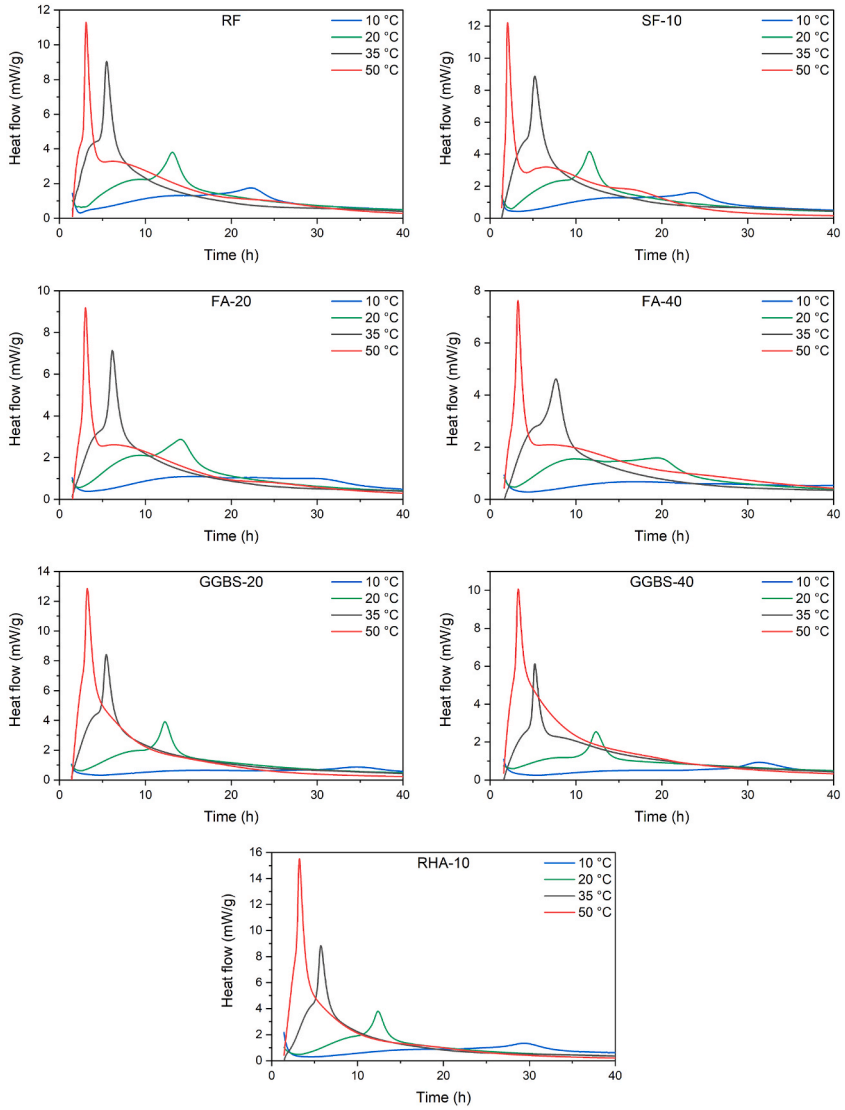

Fig. 3. Heat flow of the investigated concrete samples at different curing temperature (mW/g) normalised by the weight of binder (plotted only for the first 40 h for detailed view).

emergence of the second peak occurs when the hydration reaction of C_2S phase accelerates, causing a resurgence in the heat evolution rate. Typically, the second peak appears to surpass that of the first peak due to the cumulative heat produced by the hydration of both C_3S and C_2S phases which is greater than that produced solely by C_3S [11,80].

The renewal of C_3A dissolution, affected by gypsum and sulphate depletion, is responsible for the broadening of the main peak [21, 81]. The primary cause of the delay in hydration and subsequent dissolution of C_3A is the adsorption of sulphate around it, occurring after the consumption of sulphate [80–82]. The use of SCM in the system results in lower concentrations of sulphate in the solution compared with plain cement. This reduced concentration is entirely consumed before the end of the deceleration phase, indicating a rapid dissolution of C_3A and a sharper peak when using SCM in the system [81] as demonstrated in SF-10, GGBS-20, GGBS-40 and RHA-10. However, the heat peak of mixes containing FA appear broader (FA-20 and FA-40). The dilution effect of FA equivalent to the effectiveness of water-to-cement (w/c) ratio, can be a factor in this peak widening [71,82].

The cumulative hydration heat of the studied samples (total heat of hydration) increased with time (Fig. 2b). The control samples exhibited the highest cumulative heat. Within the authors' expectation, this may be attributed to the renewal of C_3A dissolution, resulting in a broader heat peak and causing the cumulative heat of the control samples to appear higher as the age progresses. In this connection, it is worth noting that a higher heat flow of hydration does not inevitably imply a higher cumulative heat of hydration [83].

Noticeable variations in heat flow and cumulative heat were observed in the studied samples when exposed to different temperatures. Fig. 3 shows that the hydration and pozzolanic reactions were promoted by higher temperatures and decreased by lower temperatures.

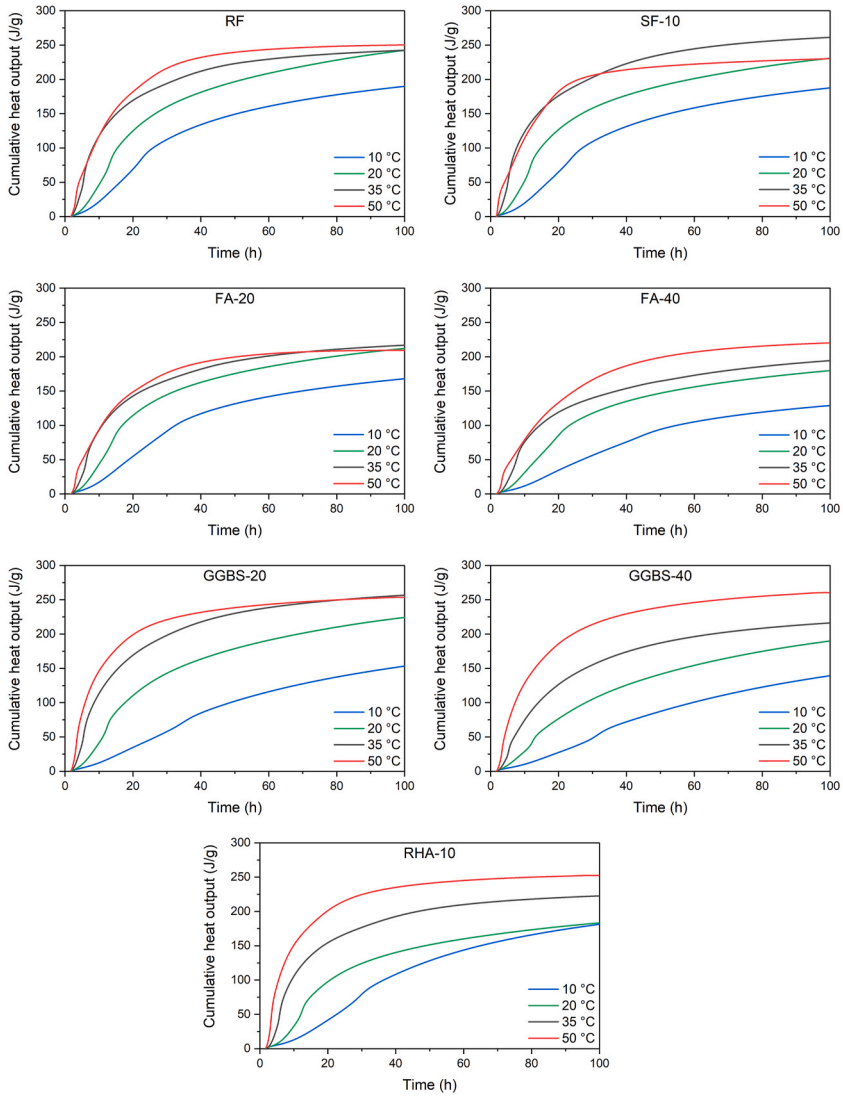

Fig. 4. Cumulative heat of all mixes at different curing temperature (mW/g) normalised by the weight of the binder.

As it is presented in Fig. 3, the higher the temperature, the higher and earlier the hydration peak achieved, regardless of the mix compositions. The higher temperature tends to accelerate the reaction activity by promoting the consumption of CH [14]. Furthermore, the peak curve tends to be sharper with higher temperatures, indicating a rapid dissolution of C_3A [84].

Since pozzolanic materials participate in forming different hydrated products, they tend to show different sensitivities to temperature than cement [85]. Mixes containing RHA exhibited the highest peak (at 50 °C) due to its high silicate composition and irregular particle shape, facilitating water adsorption, a process that is promoted by higher temperatures [53,86]. However, the higher reaction rate induced at an early age, due to a higher curing temperature, can adversely affect the hydration rate at a later age. The microstructure of the hydration products tends to be thicker with higher temperatures, which restricts the mobility of free water between them [87]. As a result, the reaction is controlled by a diffusion process that leads to a retardation of the reaction rate and a decrease in the ultimate level of hydration at a later period (Fig. 4) [16,88]. It appears that the cumulative heat over time of samples placed at higher temperatures starts to gradually approach that of samples placed at lower temperatures. This is called the ''crossover effect'' and will be discussed in the next section. A similar phenomenon has been observed by Boha et al. [16]. In general, the negative impacts of elevated temperature were alleviated through increased substitution levels with SCM, owing to their chemical and physical effects that contribute to the formation of additional C-S-H phase [13–16].

3.3. Strength development

Fig. 5 illustrates the results of strength development, with standard deviation, for all SCC specimens with various SCMs at different temperatures of curing. Since the compressive strength of concrete is primarily attributed to hydrated cement, it is commonly considered as indication of concrete performance [26,27]. It is clear that the improvement in strength is proportional to the hydration or pozzolanic reaction. When the reaction rate is high, the initial strength development will be increased, whereas the strength gain rate will deteriorate when the hydration reaction rate is low. Heat curing affects the properties of each material in a distinct manner. At standard curing temperatures, the control specimens with cement attained strength more rapidly than the other specimens, except those containing 10 % SF. The reason for this lies in the particle properties of RHA [78,79] and the slow pozzolanic reaction of FA and GGBS, primarily occurring with hydrated CH [10,72,89,90]. In contrast, SF exhibits high pozzolanic properties due to its high content of amorphous silicate and large surface area, leading to an increase in the strength of the early-age concrete [14]. In the later stages, concrete containing pozzolanic materials tends to exhibit a continuous strength gain due to the presence of more C-S-H. This leads to the refined microstructure within the concrete and is accountable for strength improvement by filling the voids in the matrix [13,15,20,72,91]. This will be discussed in greater detail in the next section.

The initial strength was improved owing to the fastened hydration and pozzolanic reactions at high temperatures, specifically at 35 °C and 50 °C for the clinker. The formation of C-S-H, primarily accountable for strength development in concrete, is formed in a faster manner at higher temperatures [86,88]. Nevertheless, this could detrimentally impact and reduce the later-age strength of concrete. This can be explained by the fact that the high curing temperature expedites hydration and leads to a heterogeneity of hydration products, causing the creation of an extensive network of pores. This phenomenon is referred to as the crossover effect [92]. Similar trends have been found in other studies [14,19,93,94].

The crossover effect, first reported by McIntosh [95], is due to the rapid reaction, which causes a high concentration and heterogeneous hydration products around the cement particles. This leads to internal stress and, as a result, large pores are generated [92,96]. Furthermore, the concentration of hydration products prevents the surrounded cement particles from continuing to be hydrated at a later age. This can explain why the concrete has lower hydration and strength at a later age when it is cured at a high temperature at an early age. It was revealed that the materials exhibiting lower pozzolanic reactions were relatively less susceptible to the negative effects of higher curing temperatures. For example, the transition point between 20 and 50 °C took place at 14 days for the control specimens, earlier than for other specimens containing SCM. This observation is in agreement with those reported elsewhere [14,19,29]. It is thought that the presence of a dense C-S-H, formed during initial stages as a result of the high curing temperature, led to a

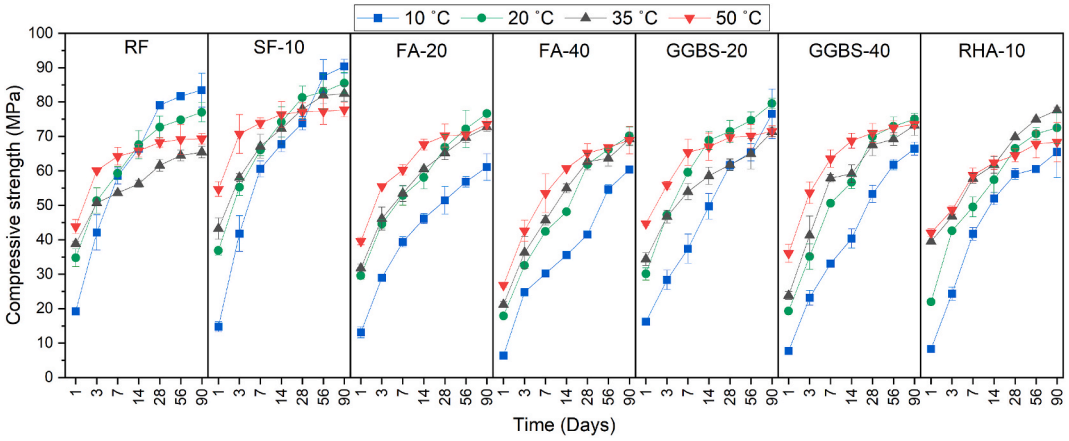

Fig. 5. Strength development of the SCC mixes cured at different temperature as a function of the curing age. Error bars represent the standard deviation.

coarser pore network in the microstructure of control concrete [87]. At a later age, the control specimens experienced low strength development at high curing temperatures due to the insufficient amount of hydration products formed at a later age, which were not sufficient to adequately fill the pores [87,88]. Even though the samples containing SF exhibited a higher reaction compared to control concrete, the detrimental effect of a high curing temperature was less significant at a later age on the samples containing SF. This was attributed to the small particle size of SF, which could improve the packing properties by efficiently filling the voids, known as micro-aggregate filling effects [14]. Samples incorporating rice husk ash (RHA) appeared to be less influenced by the negative effects, possibly due to the internal curing effect it induces, facilitating continuous hydration [78,79]. As a consequence of the gradual pozzolanic reaction in FA and GGBS concrete, the resulting C-S-H can plug the pores at later age when exposed to high temperatures [20,85]. This indicates that incorporating SCMs with cement in the binder can improve the concrete microstructure, providing protection against the harmful impact of the temperature on pore development.

In the case of a low curing temperature (10 °C), all concrete specimens exhibited slower strength development than those cured at a higher temperature. However, strength progressively increased over time. As an illustration, the compressive strength of control specimens surpassed that of those cured at a higher temperature (50 °C) starting from 14 days onwards. This was due to a slow reaction in strength gain, which led to a more uniform distribution of hydration [88,97]. In comparison to control concrete specimens, the specimens containing SF exhibit a slower rate of strength development during the initial seven days at low curing temperatures. However, from day seven onward, the strength of the specimens containing SF exceeded that of the control specimens. It was observed that the specimens incorporating FA or GGBS experienced slower strength gain over time compared with control specimens. This is possibly due to the slow hydration of cement clinker at low temperatures, which consequently affects the pozzolan, causing it to begin to react with (CH) at a later stage. The irregularly shaped particles of RHA, which facilitate water absorption and induce the reaction, deteriorate in their absorption capacity at low curing temperatures. This can explain the slow strength of the samples containing RHA.

Therefore, it could be verified that SCC specimens containing SCM, when cured at low curing temperatures, gained strength compared at lower rates. This delay in strength development is unfavourable for application in fast-track construction. In contrast, the control specimens which contain cement with no replacement with SCM exhibited a faster rate of strength development than the vibrated concrete specimen when exposed to low temperatures [19]. Despite both concrete types having a low initial heat of hydration, the reaction progresses more rapidly in SCC as it has a reduced amount of coarse aggregate, which serves as an impediment to the reaction. Additionally, the substantial amount of paste present in SCC expedited the process of strength improvement [98].

To gain more insight into the influences of different curing temperatures on the behaviour of SCC compressive strength, the compressive strength development can be expressed as a ratio (strength gain at any temperature/strength gain at 20 °C). Fig. 6 illustrates how the examined specimens respond (sensitivity) to variations in curing temperature. In general, at high curing temperatures (35 and 50 °C), there was a decline in the strength ratio over time. This decline was observed to cross the strength ratio of specimens cured at a standard curing temperature, which can be attributed to the previously mentioned crossover effect. The decline in strength ratio was delayed more with specimens containing FA, GGBS, RHA, SF, and cement with no replacement, respectively. This is due to the allowable replacement levels of FA and GGBS and the stored water in RHA particles [10,78,79]. Conversely, at a low curing temperature (10 °C), the trend was different. As the specimens aged, the strength ratio of those cured at 10 °C increased gradually and required some time to approach the strength level of specimens cured at a standard temperature. This prolonged duration became increasingly apparent in specimens containing FA, GGBS, RHA, SF, and cement with no replacement.

3.4. Porosity

To gain a better understanding of how curing temperature influences the microstructure of SCC, the porosity of the concrete was investigated, and the results were verified using standard deviation values (Fig. 7), since it directly affects the microstructure and robustness of the SCC [65]. The pore structure of the samples is refined with age, and the enhancement ratio tends to be lower when the concrete is cured at a high temperature. At an early age, the open porosity of hardened concrete exposed to a high curing temperature

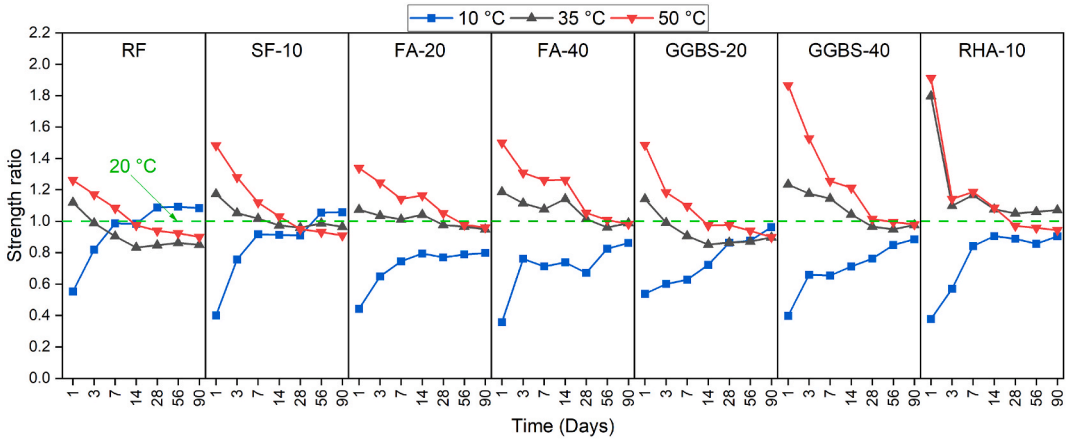

Fig. 6. Strength development ratio values of the SCC mixes at different temperatures (10, 35 and 50 °C) compared to those cured at a standard temperature (20 °C).

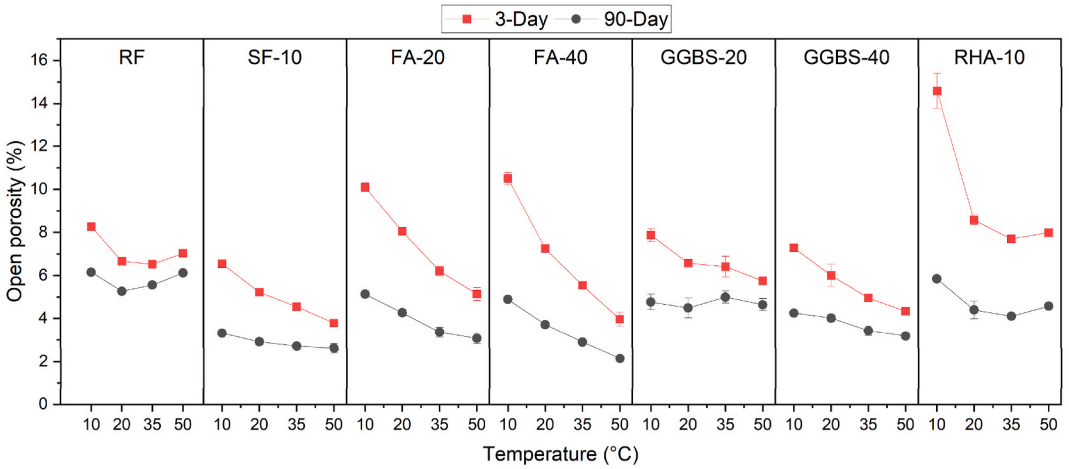

Fig. 7. Average open porosity values of the SCC mixes at different curing temperatures at 3 and 90 days of age. Error bars represent the standard deviation.

generally decreased. The higher temperatures expedited the hydration and pozzolanic reaction of the clinker, resulting in an increase in C-S-H phase content, which in turn tended to make the concrete microstructure less porous than the specimen exposed to 20 °C [14, 99]. Therefore, it could be verified that initial higher curing temperatures decreased the porosity and refined the pore structure of the concrete. Despite the initial increase in C-S-H phase content, the hydration product tended to be unevenly distributed due to the initial elevated curing temperature, which in turn hindered further hydration reactions as indicated before. Therefore, an insufficient amount of hydration products formed at a later age, which were unable to adequately fill the pores, resulting in poor refining of pore structure [86–88,99].

In the case of a low curing temperature (10 °C), the microstructure was less refined, and the open porosity was higher due to the slow formation of hydration products. However, the slow formation of hydration products tended to be uniform and refined the pore structure at a later age [88,97,99]. Using SCMs decreased the porosity and refined the pore structure of the concrete at a later age owing to their additional C-S-H formation through the pozzolanic reaction with cement, along with their beneficial physical properties. The strength increase, defined by the Strength ratio in Equation (1), is directly proportional to the refinement of the pores, denoted by the Porosity ratio in Equation (2), as illustrated in Fig. 8.

$$Strength\ ratio = \left(\left(\frac{Strength\ at\ 90\ days - Strength\ at\ 3\ days}{Strength\ at\ 3\ days} \right) \times 100 \right) \tag{1}$$

$$Porosity\ ratio = \left(\left(\frac{Porosity\ at\ 90\ days - Porosity\ at\ 3\ days}{Porosity\ at\ 3\ days} \right) \times 100 \right) \tag{2}$$

Specimens containing RHA exhibited lower pore volumes at a later age due to the stored water in the pores of RHA particles,

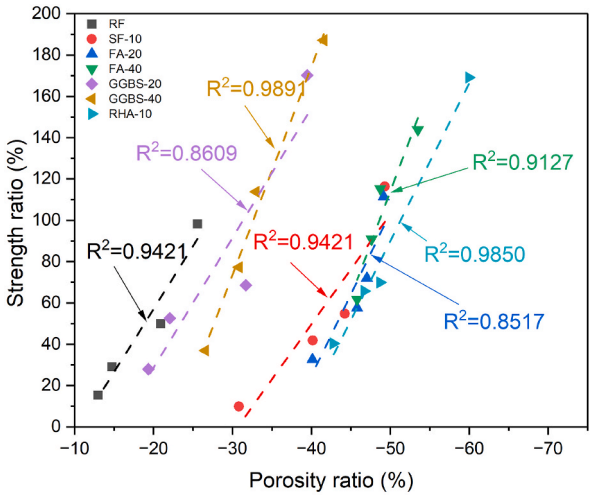

Fig. 8. Correlation between pore refinement (porosity ratio) and strength development (strength ratio) of the investigated mixes.

facilitating additional C-S-H formation, which could occupy the voids in the matrix.

3.5. Prediction of the compressive strength development

The first step to predicting the concrete strength at any age at different curing temperatures is by calculating the apparent activation energy (E_a) that is necessary for determining the equivalent age (t_e) of the concrete. Calculation of the activation energy value of the specimens involved the method of analysis outlined in ASTM C1074- 2019 [100].

Due to different mix proportion of SCC compared to conventional concrete, it is recommended to calculate E_a based on concrete samples instead of corresponding mortar suggested for conventional concrete. This is to enhance the accuracy as adopted in Refs. [19,37,41,85,101,102]. This includes fitting Equation (3) based on the outcome of strength improvement of the specimens at each curing temperature to deduce the essential constants needed for calculating the apparent activation energy.

$$S = \frac{S_u k(t - t_0)}{1 + k(t - t_0)} \tag{3}$$

In Equation (3), S denotes the strength development of the concrete (MPa) at age t, S_u represent the ultimate compressive strength of the SCC samples (MPa), k denotes the rate constant (1/day), t stands for the test age of the concrete (days), t_0 signifies the starting age assumed for concrete's strength development (days). The required constants are summarised in Table 4.

In order to predict the compressive strength development of the studied concrete specimens, it is essential to calculate the equivalent age (t_e) using the equation [103].

$$t_e = \sum_t e^{-\frac{E_a}{R}\left(\frac{1}{T} - \frac{1}{T_r}\right)} \bullet \Delta t \tag{4}$$

E_a represents the apparent activation energy (J/mol), R stands for the gas constant (J/Kmol), whereas T and T_r denotes the temperature of the concrete and reference temperature, respectively in Kelvin, Δt signifies the duration of curing period (days).

To calculate E_a, the data is presented as a plot of the natural logarithm of k ($\ln(k)$) with respect to the reciprocal of absolute temperature ($\frac{1}{T}$) as recommended in ASTM C1074- 2019 [100]. Subsequently, regression analysis was carried out by fitting a best-fit straight line through the given points (see Fig. 9). The ratio $\frac{E_a}{R}$ was determined from the negative slope of the lines. The apparent activation energy of the examined specimens is listed in Table 4.

Table 4 shows the values of E_a for the samples analysed. The finding revealed an increase in E_a for concrete containing SF, whereas a decrease was observed for concrete with FA, compared to control concrete mix. The findings align with the results of various studies reported in the literature [21,75]. Due to the high pozzolanic activity of SF [10], owing to its chemical and physical properties, the

Table 4
Regression constants for strength development of the studied samples and their values of apparent activation energy.

Mix ID	T (°C)	S_u (MPa)	k (1/day)	t_0 (days)	R^2	E_a (KJ/mol)
RF	10	86.48	0.30	1.52E-08	0.995	37.34
	20	75.74	0.73	1.73E-12	0.976	
	35	62.82	1.44	2.91E-09	0.915	
	50	69.17	2.21	0.21	0.992	
SF-10	10	90.46	0.27	0.20	0.981	45.50
	20	84.56	0.66	4.01E-13	0.981	
	35	80.67	0.98	1.48E-11	0.960	
	50	77.67	3.58	0.34	0.998	
FA-20	10	60.72	0.27	7.22E-11	0.989	25.46
	20	72.63	0.52	9.19E-09	0.934	
	35	69.78	0.67	9.39–10	0.954	
	50	71.91	1.14	1.14E-11	0.971	
FA-40	10	60.18	0.14	6.34E-08	0.934	25.62
	20	70.16	0.25	2.05E-11	0.965	
	35	68.05	0.36	3.53E-10	0.980	
	50	68.97	0.56	2.85E-13	0.994	
GGBS-20	10	76.01	0.16	1.41E-08	0.964	36.63
	20	77.74	0.55	4.62E-10	0.985	
	35	66.07	0.89	8.52E-11	0.926	
	50	70.87	1.56	4.24E-14	0.977	
GGBS-40	10	70.37	0.12	5.85E-09	0.985	40.26
	20	77.09	0.27	3.47E-13	0.988	
	35	72.6	0.46	1.82E-12	0.985	
	50	73.89	0.92	1.99E-11	0.999	
RHA-10	10	67.42	0.24	4.41E-01	0.997	32.70
	20	72.22	0.40	1.59E-11	0.976	
	35	73.16	0.79	2.03E-09	0.868	
	50	66.69	1.32	2.98E-11	0.927	

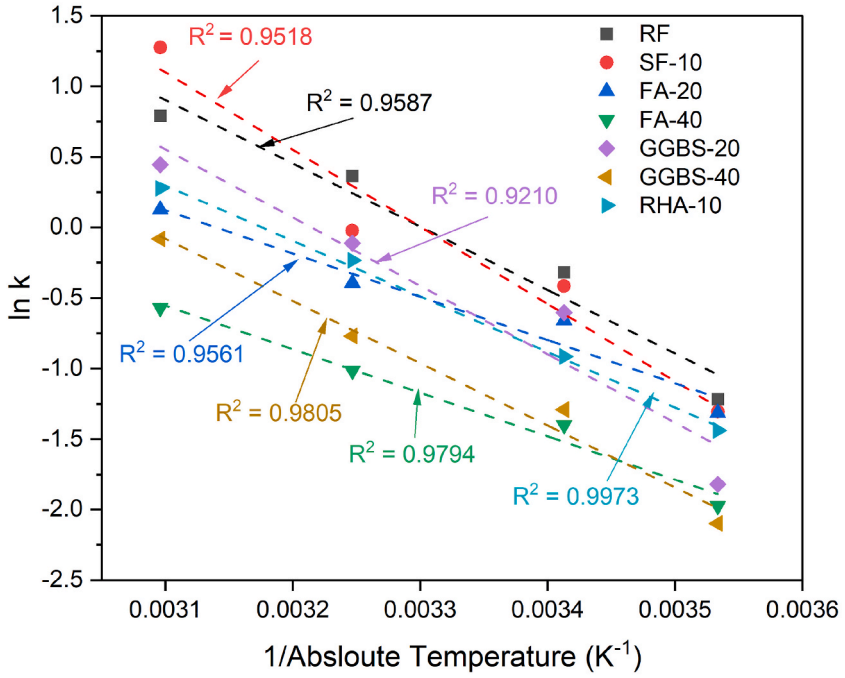

Fig. 9. Variation of "ln(k)'' based reciprocal of absolute temperature "1/T''.

hydration process of the binder with SF tends to be primarily controlled by chemical reactions. Consequently, substituting SF for cement in the concrete raised the E_a value. On the other hand, when using FA in the concrete, the chemical reaction initially drives the hydration for limited time, but it is then primarily dominated by the diffusion process [71,75]. The hydration process primarily regulated by diffusion seems to result in a lower E_a value compared to the one governed by chemical reactions [75]. As a result, using fly ash in the binder for concrete led to a reduction in E_a value. In contrast, GGBS is hydraulic material with a composition close to that of Portland cement, enabling it to independently react with water. Therefore, E_a values of samples with GGBS and control samples show no distinctive difference [75]. The complex hydration mechanisms of RHA as previously described, produce a unique E_a value. In this study, E_a values of high-strength SCC samples appear to be lower than those found in the existing literature [19] for normal concrete. The reason behind this observation may stem from the distinct hydration kinetics and initial strength characteristics of the SCC samples in this study, attributed to their high powder content, which had possibly reduced water absorption necessary for the binder hydration at later stages [101,104].

To predict the strength development of SCC specimens at any curing temperature, the equivalent age (t_e) determined by Equation (4) can be substituted for test age t in Equation (3), using the relevant constants S_u, k and t_0 which are determined at the standard curing temperature. Fig. 10 illustrates the calculated strength estimation of the examined specimens. As previously observed, the strength development of SCC specimens was significantly influenced by the SCM in the blended cement and the curing temperature. These factors had a significant effect on the trend of strength estimation for the studied specimens. At a low curing temperature, the early-age strength estimation of (RF) and (SF-10) was higher than the actual strength, but it was underestimated as the age of the concrete increased. On the contrary, the strength of the specimens containing FA or GGBS was overestimated, particularly with a greater level of replacement with cement through the test period. This is primarily because of the gradual pozzolanic reaction observed in FA and GGBS materials. At higher curing temperatures, the overestimate for the strength was more pronounced in (RF) compared with other samples containing SCM, as was evident from the crossover effect that took place earlier in (RF). The accuracy of the comparison between predicted and experimental compressive strength is presented in Fig. 11.

4. Conclusion

This study investigated the influences of maturity on the hydration reaction process and development of compressive strength in high-strength SCC with various SCMs as partial Portland cement substitutions, and the following conclusions were drawn.

- The addition of SF and RHA in SCC decreased workability, while the addition of FA and GGBS enhanced workability. All of these findings demonstrated the variation in water demand caused by the fineness of SCMs with cement.
- The specimens incorporating SF were more pronounced in reaction and achieved higher and earlier peak temperatures than the other specimens containing RHA, FA or GGBS. Consequently, using SF can lead to an increase initial strength of the concrete, while using RHA, FA or GGBS causes a deceleration in strength progress, but contributes to a higher level of strength gain in the long term.

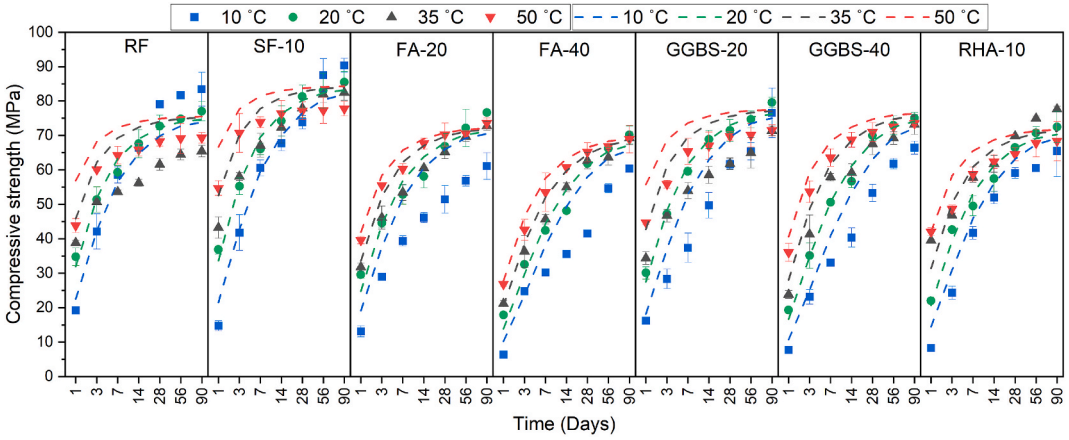

Fig. 10. Estimation of the compressive strength development of the studied samples as a function of the age and the curing temperature. Markers represent the experimental data, and dotted lines represent the predicted strength values. Error bars represent the standard deviation.

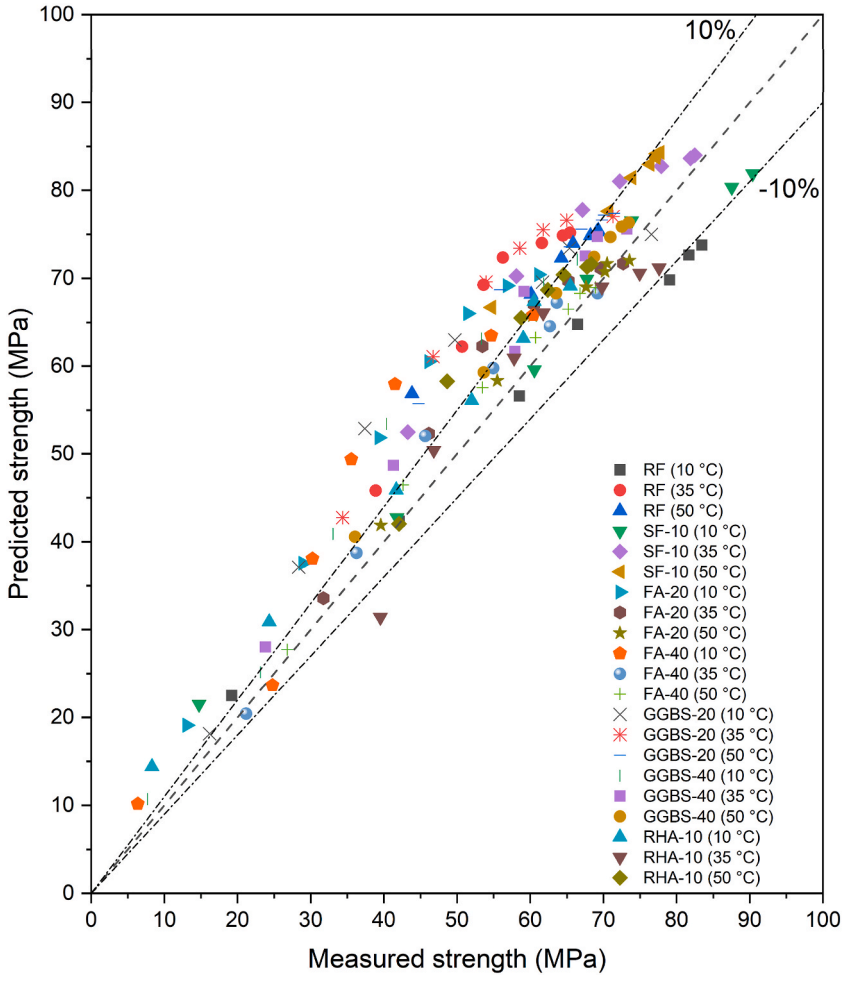

Fig. 11. Accuracy of predicted and experimental compressive strength values.

- High curing temperatures can expedite the hydration reaction associated with progress in early-age concrete strength, but concurrently could lead to delayed strength progress at a late age. This detrimental effect can possibly be mitigated by using SCM in blended cement. The occurrence of a crossover effect was noticeably delayed with inclusion of FA, GGBS, RHA and SF, respectively in the studied specimens.
- At low curing temperatures, the hydration and pozzolanic reactions deteriorated, causing a slow gain in concrete strength. However, strength continued to develop over time. The SCC specimens incorporating RHA, FA or GGBS experienced slower strength gain over time compared with control specimens. Despite the potential enhancement in the compressive strength of the concrete with the addition of SF after 7 days, the drawback lies in the slow initial strength development of SCC with SCM, which is not ideal for fast-track construction.
- The concrete microstructure tended to be denser and less porous at high curing temperatures compared with the specimens cured at standard or low curing temperatures. However, this can lead to a poor rate of refinement of the pore structure in the long term. Conversely, the microstructure was less dense and more porous at a low curing temperature, but with a high rate of enhancement in pores of the structure in the long term.
- The estimation of the strength development of SCC by the maturity method was significantly influenced by SCMs in the blended cement and the curing temperature. Overestimation was observed more at low curing temperatures in specimens containing FA or GGBS, particularly with a higher replacement level as well as in specimens containing RHA. On the other hand, overestimation of strength was more pronounced in control specimens at high curing temperatures.

CRediT authorship contribution statement

Ayman Almutlaqah: Writing – original draft, Investigation, Formal analysis, Data curation, Conceptualization. **Abdullah Alshahrani:** Investigation, Formal analysis. **Riccardo Maddalena:** Writing – review & editing, Supervision, Methodology. **Sivakumar Kulasegaram:** Writing – review & editing, Supervision, Project administration, Methodology.

Declaration of competing interest

The authors declare that they have no known competing financial interests or personal relationships that could have appeared to influence the work reported in this paper.

Data availability

Data will be made available on request.

References

[1] M. Okamura, H, Ouchi, Self-compacting Concrete.pdf, J. Adv. Concr. Technol. 1 (2003) 5–15, https://doi.org/10.3151/jact.1.5.
[2] M.S. Ashtiani, A.N. Scott, R.P. Dhakal, Mechanical and fresh properties of high-strength self-compacting concrete containing class C fly ash, Constr Build Mater 47 (2013) 1217–1224, https://doi.org/10.1016/j.conbuildmat.2013.06.015.
[3] S. Assié, G. Escadeillas, V. Waller, Estimates of self-compacting concrete “potential” durability, Constr Build Mater 21 (2007) 1909–1917, https://doi.org/10.1016/j.conbuildmat.2006.06.034.
[4] X. An, Q. Wu, F. Jin, M. Huang, H. Zhou, C. Chen, C. Liu, Rock-filled concrete, the new norm of SCC in hydraulic engineering in China, Cem. Concr. Compos. 54 (2014) 89–99, https://doi.org/10.1016/j.cemconcomp.2014.08.001.
[5] A. Mohan, K.M. Mini, Strength and durability studies of SCC incorporating silica fume and ultra fine GGBS, Constr Build Mater 171 (2018) 919–928, https://doi.org/10.1016/j.conbuildmat.2018.03.186.
[6] N. Gupta, R. Siddique, Sustainable and greener self-compacting concrete incorporating industrial by-products : a review, Cleaner Production 284 (2021), https://doi.org/10.1016/j.jclepro.2020.124803.
[7] M. Benaicha, X. Roguiez, O. Jalbaud, Y. Burtschell, A. Hafidi, Influence of silica fume and viscosity modifying agent on the mechanical and rheological behavior of self compacting concrete, Constr Build Mater 84 (2015) 103–110, https://doi.org/10.1016/j.conbuildmat.2015.03.061.
[8] P. Ramanathan, I. Baskar, P. Muthupriya, R. Venkatasubramani, Performance of self-compacting concrete containing different mineral admixtures, KSCE J. Civ. Eng. 17 (2013) 465–472, https://doi.org/10.1007/s12205-013-1882-8.
[9] K.P. Sethy, D. Pasla, U. Chandra Sahoo, Utilization of high volume of industrial slag in self compacting concrete, J. Clean. Prod. 112 (2016) 581–587, https://doi.org/10.1016/j.jclepro.2015.08.039.
[10] B. Lothenbach, K. Scrivener, R.D. Hooton, Supplementary cementitious materials, Cem Concr Res 41 (2011) 1244–1256, https://doi.org/10.1016/j.cemconres.2010.12.001.
[11] J. Beaudoin, I. Odler, Hydration, Setting and Hardening of Portland Cement, fifth ed., Elsevier Ltd., 2019 https://doi.org/10.1016/B978-0-08-100773-0.00005-8.
[12] M. Thomas, Supplementary cementing materials in concrete. https://doi.org/10.1201/b14493, 2013.
[13] V. Kannan, Strength and durability performance of self compacting concrete containing self-combusted rice husk ash and metakaolin, Constr Build Mater 160 (2018) 169–179, https://doi.org/10.1016/j.conbuildmat.2017.11.043.
[14] Z. Zhang, B. Zhang, P. Yan, Hydration and microstructures of concrete containing raw or densified silica fume at different curing temperatures, Constr Build Mater 121 (2016) 483–490, https://doi.org/10.1016/j.conbuildmat.2016.06.014.
[15] Q. Wang, J.J. Feng, P.Y. Yan, An explanation for the negative effect of elevated temperature at early ages on the late-age strength of concrete, J. Mater. Sci. 46 (2011) 7279–7288, https://doi.org/10.1007/s10853-011-5689-z.
[16] M. Boha, M.T. Palou, E. Kuzielova, R. Novotny, The effect of curing temperature on the hydration of binary Portland cement, J. Therm. Anal. Calorim. (2016) 1301–1310, https://doi.org/10.1007/s10973-016-5395-9.
[17] S.U. Khan, M.F. Nuruddin, T. Ayub, N. Shafiq, Effects of different mineral admixtures on the properties of fresh concrete, Sci. World J. 2014 (2014), https://doi.org/10.1155/2014/986567.
[18] J. Liu, Y. Li, P. Ouyang, Y. Yang, Hydration of the silica fume-Portland cement binary system at lower temperature, Constr Build Mater 93 (2015) 919–925, https://doi.org/10.1016/j.conbuildmat.2015.05.069.

[19] M. Soutsos, F. Kanavaris, M. Elsageer, Accuracy of maturity functions ' strength estimates for fly ash concretes cured at elevated temperatures, Constr Build Mater 266 (2021) 121043, https://doi.org/10.1016/j.conbuildmat.2020.121043.
[20] F. Han, Z. Zhang, Hydration , mechanical properties and durability of high-strength concrete under different curing conditions, J. Therm. Anal. Calorim. 132 (2018) 823–834, https://doi.org/10.1007/s10973-018-7007-3.
[21] G. Xu, Q. Tian, J. Miao, J. Liu, Early-age hydration and mechanical properties of high volume slag and fly ash concrete at different curing temperatures, Constr Build Mater 149 (2017) 367–377, https://doi.org/10.1016/j.conbuildmat.2017.05.080.
[22] J. Vilar, C.M. Vázquez-herrero, C. Javier, R. Meli, C. Aire, Statistical validation of new maturity functions for high-strength self-consolidating concrete mixes, Constr Build Mater 168 (2018) 931–945, https://doi.org/10.1016/j.conbuildmat.2018.02.074.
[23] S. Teixeira, A. Santilli, I. Puente, Demoulding vertical elements : recommendations for apply maturity functions, Constr Build Mater 145 (2017) 392–401, https://doi.org/10.1016/j.conbuildmat.2017.04.006.
[24] M. Soutsos, A. Hatzitheodorou, J. Kwasny, F. Kanavaris, Effect of in situ temperature on the early age strength development of concretes with supplementary cementitious materials, Constr Build Mater 103 (2016) 105–116, https://doi.org/10.1016/j.conbuildmat.2015.11.034.
[25] T.A. Yikici, H.R. Chen, Use of maturity method to estimate compressive strength of mass concrete, Constr Build Mater 95 (2015) 802–812, https://doi.org/10.1016/j.conbuildmat.2015.07.026.
[26] C. Vu, O. Plé, J. Weiss, D. Amitrano, Revisiting the concept of characteristic compressive strength of concrete, Constr Build Mater 263 (2020) 120126, https://doi.org/10.1016/j.conbuildmat.2020.120126.
[27] Q. Xu, J. Hu, J.M. Ruiz, K. Wang, Z. Ge, Isothermal calorimetry tests and modeling of cement hydration parameters, Thermochim. Acta 499 (2010) 91–99, https://doi.org/10.1016/j.tca.2009.11.007.
[28] T. Boubekeur, K. Ezziane, E. Kadri, Estimation of mortars compressive strength at different curing temperature by the maturity method, Constr Build Mater 71 (2014) 299–307, https://doi.org/10.1016/j.conbuildmat.2014.08.084.
[29] M. Soutsos, A. Hatzitheodorou, F. Kanavaris, J. Kwasny, Effect of temperature on the strength development of mortar mixes with GGBS and fly ash, Mag. Concr. Res. 69 (2017) 787–801, https://doi.org/10.1680/jmacr.16.00268.
[30] J.K. Kim, S.H. Han, Y.C. Song, Effect of temperature and aging on the mechanical properties of concrete: Part I. Experimental results, Cem Concr Res 32 (2002) 1087–1094, https://doi.org/10.1016/S0008-8846(02)00744-5.
[31] S. Mengxiao, W. Qiang, Z. Zhikai, Comparison of the properties between high-volume fly ash concrete and high-volume steel slag concrete under temperature matching curing condition, Constr Build Mater 98 (2015) 649–655, https://doi.org/10.1016/j.conbuildmat.2015.08.134.
[32] A. Vollpracht, M. Soutsos, F. Kanavaris, Strength development of GGBS and fly ash concretes and applicability of fib model code's maturity function – a critical review, Constr Build Mater 162 (2018) 830–846, https://doi.org/10.1016/j.conbuildmat.2017.12.054.
[33] C. Shi, Z. Wu, K. Lv, L. Wu, A review on mixture design methods for self-compacting concrete, Constr Build Mater 84 (2015) 387–398, https://doi.org/10.1016/j.conbuildmat.2015.03.079.
[34] B. Felekoğlu, S. Türkel, B. Baradan, Effect of water/cement ratio on the fresh and hardened properties of self-compacting concrete, Build. Environ. 42 (2007) 1795–1802, https://doi.org/10.1016/j.buildenv.2006.01.012.
[35] P. Dinakar, K.P. Sethy, U.C. Sahoo, Design of self-compacting concrete with ground granulated blast furnace slag, Mater. Des. 43 (2013) 161–169, https://doi.org/10.1016/j.matdes.2012.06.049.
[36] J.L. García Calvo, M.C. Alonso, L. Fernández Luco, M. Robles Velasco, Durability performance of sustainable self compacting concretes in precast products due to heat curing, Constr Build Mater 111 (2016) 379–385, https://doi.org/10.1016/j.conbuildmat.2016.02.097.
[37] M.N. Soutsos, G. Turu, K. Owens, J. Kwasny, S.J. Barnett, P.A.M. Basheer, Maturity testing of lightweight self-compacting and vibrated concretes, Constr Build Mater 47 (2013) 118–125, https://doi.org/10.1016/j.conbuildmat.2013.04.045.
[38] G. Barluenga, C. Guardia, J. Puentes, Effect of curing temperature and relative humidity on early age and hardened properties of SCC, Constr Build Mater 167 (2018) 235–242, https://doi.org/10.1016/j.conbuildmat.2018.02.029.
[39] H.W. Reinhardt, M. Stegmaier, Influence of heat curing on the pore structure and compressive strength of self-compacting concrete (SCC), Cem Concr Res 36 (2006) 879–885, https://doi.org/10.1016/j.cemconres.2005.12.004.
[40] A. Boukhelkhal, L. Azzouz, S. Kenai, E. Kadri, B. Benabed, Combined effects of mineral additions and curing conditions on strength and durability of self-compacting mortars exposed to aggressive solutions in the natural hot-dry climate in North African desert region, Constr Build Mater 197 (2019) 307–318, https://doi.org/10.1016/j.conbuildmat.2018.11.233.
[41] M. Benaicha, Y. Burtschell, A. Ha, Prediction of compressive strength at early age of concrete – application of maturity, J. Build. Eng. 6 (2016) 119–125, https://doi.org/10.1016/j.jobe.2016.03.003.
[42] WAP, Rice production by country - world agricultural production 2020/2021. http://www.worldagriculturalproduction.com/crops/rice.aspx, 2021.
[43] E. Molaei Raisi, J. Vaseghi Amiri, M.R. Davoodi, Mechanical performance of self-compacting concrete incorporating rice husk ash, Constr Build Mater 177 (2018) 148–157, https://doi.org/10.1016/j.conbuildmat.2018.05.053.
[44] EN 197-1, Cement - Part 1: Composition, Specifications and Conformity Criteria for Common Cements Ciment, EUROPEAN COMMITTEE FOR STANDARDIZATION, 2019.
[45] BS EN 934-2, Admixtures for Concrete, Mortar and Grout, BSI Standards, 2009, pp. 3–36, https://doi.org/10.1016/B978-075065686-3/50280-9.
[46] A. Alshahrani, T. Cui, A. Almutlaqah, S. Kulasegaram, Designing sustainable high-strength self-compacting concrete with high content of supplementary cementitious materials, European Journal of Environmental and Civil Engineering 0 (2023) 1–20, https://doi.org/10.1080/19648189.2023.2279563.
[47] M. Gesoğlu, E. Güneyisi, E. Özbay, in: Properties of Self-Compacting Concretes Made with Binary , Ternary , and Quaternary Cementitious Blends of Fly Ash , Blast Furnace Slag , and Silica Fume, vol. 23, 2009, pp. 1847–1854, https://doi.org/10.1016/j.conbuildmat.2008.09.015.
[48] BS 12350-8, Part 8: self-compacting concrete — slump- flow test, BSI Standards (2009).
[49] BS EN 12350-12, Part 12: Self-Compacting Concrete — J-Ring Test, BSI Standards, 2010.
[50] calmetrix, I-Cal 8000 HPC _ calmetrix. https://www.calmetrix.com/i-cal-8000-hpc, 2023.
[51] ASTM C1702, Standard Test Method for Measurement of Heat of Hydration of Hydraulic Cementitious Materials Using Isothermal Conduction, ASTM Standards, 2017, https://doi.org/10.1520/C1702-17.
[52] S. Muthukrishnan, S. Gupta, H.W. Kua, Application of rice husk biochar and thermally treated low silica rice husk ash to improve physical properties of cement mortar, Theor. Appl. Fract. Mech. 104 (2019) 102376, https://doi.org/10.1016/j.tafmec.2019.102376.
[53] A.P. Vieira, R.D. Toledo Filho, L.M. Tavares, G.C. Cordeiro, Effect of particle size, porous structure and content of rice husk ash on the hydration process and compressive strength evolution of concrete, Constr Build Mater 236 (2020) 117553, https://doi.org/10.1016/j.conbuildmat.2019.117553.
[54] G. Turu'allo, Early age strength development of GGBS concrete cured under different temperatures, Civil Engineering PhD (2013) 1–583.
[55] ASTM C1897, Standard Test Methods for Measuring the Reactivity of Supplementary Cementitious Materials by Isothermal Calorimetry and Bound Water Measurements, 2020, https://doi.org/10.1520/C1897-20. ASTM C 1897, ASTM Standards.
[56] BS EN 12390-3, Testing hardened concrete - Part 3: compressive strength of test specimens, BSI Standards 38 (2009) 18.
[57] C. Gallé, Effect of drying on cement-based materials pore structure as identified by mercury intrusion porosimetry - a comparative study between oven-, vacuum-, and freeze-drying, Cem Concr Res 31 (2001) 1467–1477, https://doi.org/10.1016/S0008-8846(01)00594-4.
[58] S. Roels, J. Carmeliet, H. Hens, O. Adan, H. Brocken, R. Cerny, Z. Pavlik, C. Hall, K. Kumaran, L. Pel, R. Plagge, Interlaboratory comparison of hygric properties of porous building materials, J. Therm. Envelope Build. Sci. 27 (2004) 307–325, https://doi.org/10.1177/1097196304042119.
[59] EFNARC, in: The European Guidelines for Self-Compacting Concrete, 2005.
[60] BS EN 206-9, Part 9: Additional Rules for Self- Compacting Concrete (SCC), BSI Standards, 2010.
[61] ASTM C1621, Standard Test Method for Passing Ability of Self-Consolidating Concrete by J-Ring, ASTM Standards, 2017, https://doi.org/10.1520/C1621_C1621M-17.

[62] D. Karthik, K. Nirmalkumar, R. Priyadharshini, Characteristic assessment of self-compacting concrete with supplementary cementitious materials, Constr Build Mater 297 (2021) 123845, https://doi.org/10.1016/j.conbuildmat.2021.123845.

[63] V.T.A. Van, C. Rößler, D.D. Bui, H.M. Ludwig, Mesoporous structure and pozzolanic reactivity of rice husk ash in cementitious system, Constr Build Mater 43 (2013) 208–216, https://doi.org/10.1016/j.conbuildmat.2013.02.004.

[64] C. Lu, H. Yang, G. Mei, Relationship between slump flow and rheological properties of self compacting concrete with silica fume and its permeability, Constr Build Mater 75 (2015) 157–162, https://doi.org/10.1016/j.conbuildmat.2014.08.038.

[65] D. Chopra, R. Siddique, Kunal, Strength, permeability and microstructure of self-compacting concrete containing rice husk ash, Biosyst. Eng. 130 (2015) 72–80, https://doi.org/10.1016/j.biosystemseng.2014.12.005.

[66] M. Şahmaran, M. Lachemi, T.K. Erdem, H.E. Yücel, Use of spent foundry sand and fly ash for the development of green self-consolidating concrete, Mater. Struct. 44 (2011) 1193–1204, https://doi.org/10.1617/s11527-010-9692-7.

[67] A. Beycioglu, H. Yilmaz Aruntaş, Workability and mechanical properties of self-compacting concretes containing LLFA, GBFS and MC, Constr Build Mater 73 (2014) 626–635, https://doi.org/10.1016/j.conbuildmat.2014.09.071.

[68] A. Benli, Mechanical and durability properties of self-compacting mortars containing binary and ternary mixes of fly ash and silica fume, Struct. Concr. 20 (2019) 1096–1108, https://doi.org/10.1002/suco.201800302.

[69] S. Tavasoli, M. Nili, B. Serpoosh, Effect of GGBS on the frost resistance of self-consolidating concrete, Constr Build Mater 165 (2018) 717–722, https://doi.org/10.1016/j.conbuildmat.2018.01.027.

[70] X. Ouyang, D.A.K. Guang, Y.K. Van Breugel, Insights into the mechanisms of nucleation and growth of C – S – H on fillers, Mater. Struct. 50 (2017) 1–13, https://doi.org/10.1617/s11527-017-1082-y.

[71] M. Narmluk, T. Nawa, Effect of fly ash on the kinetics of Portland cement hydration at different curing temperatures, Cem Concr Res 41 (2011) 579–589, https://doi.org/10.1016/j.cemconres.2011.02.005.

[72] F. Deschner, F. Winnefeld, B. Lothenbach, S. Seufert, P. Schwesig, S. Dittrich, F. Goetz-neunhoeffer, J. Neubauer, Hydration of Portland cement with high replacement by siliceous fly ash, Cem Concr Res 42 (2012) 1389–1400, https://doi.org/10.1016/j.cemconres.2012.06.009.

[73] S.Y. Hong, F.P. Glasser, Alkali binding in cement pastes : Part I. The C-S-H phase, Cem Concr Res 29 (1999) 1893–1903, https://doi.org/10.1016/S0008-8846(99)00187-8.

[74] S.Y. Hong, F.P. Glasser, Alkali sorption by C-S-H and C-A-S-H gels: Part II. Role of alumina, Cem Concr Res 32 (2002) 1101–1111, https://doi.org/10.1016/S0008-8846(02)00753-6.

[75] W. Jiachun, Y. Peiyu, Y. Hongfa, in: Apparent Activation Energy of Concrete in Early Age Determined by Adiabatic Test, 2007, https://doi.org/10.1007/s11595-006-3537-9, 537–541.

[76] A.R. Jayapalan, M.L. Jue, K.E. Kurtis, Nanoparticles and apparent activation energy of Portland cement, J. Am. Ceram. Soc. 97 (2014) 1534–1542, https://doi.org/10.1111/jace.12878.

[77] J. Wang, J. Xiao, Z. Zhang, K. Han, X. Hu, F. Jiang, Action mechanism of rice husk ash and the effect on main performances of cement-based materials: a review, Constr Build Mater 288 (2021) 123068, https://doi.org/10.1016/j.conbuildmat.2021.123068.

[78] X. Luo, X. Jiang, Q. Chen, Z. Huang, An assessment method of hydration degree of Rice husk ash blended cement considering temperature effect, Constr Build Mater 304 (2021) 124534, https://doi.org/10.1016/j.conbuildmat.2021.124534.

[79] N. Van Tuan, G. Ye, K. Van Breugel, O. Copuroglu, Hydration and microstructure of ultra high performance concrete incorporating rice husk ash, Cem Concr Res 41 (2011) 1104–1111, https://doi.org/10.1016/j.cemconres.2011.06.009.

[80] J.W. Bullard, H.M. Jennings, R.A. Livingston, A. Nonat, G.W. Scherer, J.S. Schweitzer, K.L. Scrivener, J.J. Thomas, Mechanisms of cement hydration, Cem Concr Res 41 (2011) 1208–1223, https://doi.org/10.1016/j.cemconres.2010.09.011.

[81] B.M. Gassó, Impact of the Supplementary Cementitious Materials on the kinetics and microstructural development of cement hydration, PhD Thesis 6417 (2015) 154. https://infoscience.epfl.ch/record/204690/files/EPFL_TH6417.pdf%5Cn. files/148/EPFL_TH6417.pdf.

[82] K.L. Scrivener, P. Juilland, P.J.M. Monteiro, Advances in understanding hydration of Portland cement, Cem Concr Res 78 (2015) 38–56, https://doi.org/10.1016/j.cemconres.2015.05.025.

[83] I. Pane, W. Hansen, Investigation of blended cement hydration by isothermal calorimetry and thermal analysis, Cem Concr Res 35 (2005) 1155–1164, https://doi.org/10.1016/j.cemconres.2004.10.027.

[84] C. Hesse, F. Goetz-Neunhoeffer, J. Neubauer, A new approach in quantitative in-situ XRD of cement pastes: correlation of heat flow curves with early hydration reactions, Cem Concr Res 41 (2011) 123–128, https://doi.org/10.1016/j.cemconres.2010.09.014.

[85] F. Kanavaris, M. Soutsos, J.F. Chen, Enabling sustainable rapid construction with high volume GGBS concrete through elevated temperature curing and maturity testing, J. Build. Eng. 63 (2023) 105434, https://doi.org/10.1016/j.jobe.2022.105434.

[86] A.M. Gajewicz-Jaromin, P.J. McDonald, A.C.A. Muller, K.L. Scrivener, Influence of curing temperature on cement paste microstructure measured by 1H NMR relaxometry, Cem Concr Res 122 (2019) 147–156, https://doi.org/10.1016/j.cemconres.2019.05.002.

[87] E. Gallucci, X. Zhang, K.L. Scrivener, Effect of temperature on the microstructure of calcium silicate hydrate (C-S-H), Cem Concr Res 53 (2013) 185–195, https://doi.org/10.1016/j.cemconres.2013.06.008.

[88] J.I. Escalante-García, J.H. Sharp, Effect of temperature on the hydration of the main clinker phase in Portland cements: Part I, neat cements, Cem Concr Res 28 (1998) 1245–1257.

[89] J.M. Gao, C.X. Qian, H.F. Liu, B. Wang, L. Li, ITZ microstructure of concrete containing GGBS, Cem Concr Res 35 (2005) 1299–1304, https://doi.org/10.1016/j.cemconres.2004.06.042.

[90] S.K. Lim, T.C. Ling, M.W. Hussin, Strength properties of selfcompacting mortar mixed with GGBFS, Proc. Inst. Civ. Eng.: Construction Materials 165 (2012) 87–98, https://doi.org/10.1680/coma.10.00016.

[91] K. De Weerdt, M. Ben Haha, G. Le Saout, K.O. Kjellsen, H. Justnes, B. Lothenbach, Hydration mechanisms of ternary Portland cements containing limestone powder and fl y ash, Cem Concr Res 41 (2011) 279–291, https://doi.org/10.1016/j.cemconres.2010.11.014.

[92] G.J. Verbeck, R.H. Helmuth, Structures and physical properties of cement pastes, 5th International Congress on the Chemistry of Cement 13 (1968) 1–32.

[93] S.J. Barnett, M.N. Soutsos, S.G. Millard, J.H. Bungey, Strength development of mortars containing ground granulated blast-furnace slag: effect of curing temperature and determination of apparent activation energies, Cem Concr Res 36 (2006) 434–440, https://doi.org/10.1016/j.cemconres.2005.11.002.

[94] B. Lothenbach, T. Matschei, G. Möschner, F.P. Glasser, Thermodynamic Modelling of the Effect of Temperature on the Hydration and Porosity of Portland Cement, vol. 38, 2008, pp. 1–18, https://doi.org/10.1016/j.cemconres.2007.08.017.

[95] J.D. McIntosh, The effects of low-temperature curing on the compressive strength of concrete, in: RILEM Symposium on Winter Concreting, Danish Institute for Building Research, Session BII, 1956. Copenhagen.

[96] N.J. Carino, H.S. Lew, THE MATURITY METHOD: FROM THEORY TO APPLICATION, National Institute of Standards and Technology, 2001.

[97] J.J. Thomas, D. Rothstein, H.M. Jennings, B.J. Christensen, Effect of hydration temperature on the solubility behavior of Ca-, S-, Al-, and Si-bearing solid phases in Portland cement pastes, Cem Concr Res 33 (2003) 2037–2047, https://doi.org/10.1016/S0008-8846(03)00224-2.

[98] C.K. Nmai, Cold weather concreting Admixtures, Cem. Concr. Compos. 20 (2) (1998) 121–128.

[99] B. Lothenbach, F. Winnefeld, C. Alder, E. Wieland, P. Lunk, Effect of Temperature on the Pore Solution , Microstructure and Hydration Products of Portland Cement Pastes, vol. 37, 2007, pp. 483–491, https://doi.org/10.1016/j.cemconres.2006.11.016.

[100] ASTM C1074-19e1, Standard Practice for Estimating Concrete Strength by the Maturity Method Maturity Index and Maturity Method, ASTM Standards, 2019, https://doi.org/10.1520/C1074-19E01.

[101] J. Zhang, D. Cusson, P. Monteiro, J. Harvey, New perspectives on maturity method and approach for high performance concrete applications, Cem Concr Res 38 (2008) 1438–1446, https://doi.org/10.1016/j.cemconres.2008.08.001.

[102] J.K. Kim, S.H. Han, K.M. Lee, Estimation of compressive strength by a new apparent activation energy function, Cem Concr Res 31 (2001) 217–225, https://doi.org/10.1016/S0008-8846(00)00481-6.
[103] P.F. Hansen, E.J. Pedersen, in: Maturity Computer for Controlled Curing and Hardening of Concrete, 1977.
[104] Y.A. Abdel-Jawad, Estimating concrete strength using a modified maturity model, Proc. Inst. Civ. Eng.: Construction Materials 159 (2006) 33–37, https://doi.org/10.1680/coma.2006.159.1.33.